Adiabatic Behavior of Thermal Unstable Compounds Evaluated by Means of Dynamic Scanning Calorimetric (DSC) Techniques

Roberto Sanchirico
Istituto di Ricerche sulla Combustione (IRC) – Consiglio Nazionale delle Ricerche (CNR) – P.le V. Tecchio, 80 – 80125 – Napoli, Italy

DOI 10.1002/aic.14122
Published online May 16, 2013 in Wiley Online Library (wileyonlinelibrary.com)

The article investigates the possibility of obtaining reliable information on the adiabatic behavior of thermally unstable substances based on the thermokinetic data collected by differential scanning calorimetric experiments. In particular, it is developed a novel numerical algorithm which allows the estimation of the adiabatic onset temperature. Theoretical results are verified considering the thermal decomposition of dicumyl peroxide carried out under different calorimetric conditions. Encouraging results point out that the procedures developed allow the assessment of adiabatic critical parameters that are very close to the values determined during the experiments. © 2013 American Institute of Chemical Engineers *AIChE J*, 59: 3806–3815, 2013

Keywords: adiabatic onset temperature, adiabatic time to maximum rate, differential scanning calorimetry, kinetic model, dicumyl peroxide

Introduction

Over the past few years, a number of industrial accidents involving thermal explosions have been reported in the literature.[1,2] A closer look at the causes of these incidents reveals that one of the major reasons can be ascribed to the lack of knowledge of the thermal behavior of the substances involved.[3,4] This lack of knowledge has different origins. The assessment of the thermal characteristics associated with the decomposition process of an unstable compound or reacting mixture generally involves an experimental activity which is often a very difficult, time, and money consuming task. If the system under study is believed to be capable of triggering a dangerous thermal decomposition or a runaway process, a differential scanning calorimetric (DSC) Dynamic run is the first screen carried out on the system under study.[5] The successive experimental assessment procedure typically involves the execution of a series of adiabatic runs. These calorimeters are generally expensive and their use and interpretation of the results require well trained and specialized personnel. If the necessary experimental data are not available, an open literature survey or numerical evaluations (using CHETAH program, for example,[6] or other theoretical approaches[7]) are generally considered (desktop methods). Although they can give valuable indications especially during the first evaluation stage, these tools could underestimate a series of drawbacks not as rare as one might think. For example, we may consider the presence of traces of a spurious compound in a feedstock:[8,9] this system (substance + impurity) should be characterized starting from the beginning and considering the literature or numerical data on the pure compound only as a rough estimate on its reactivity. The present work investigates the possibility of determining with a sufficient approximation the behavior of the system extrapolating the results obtained with a set of few DSC dynamic runs, to different (in particular adiabatic) conditions. This approach would be particularly useful for small or medium factories, which generally are not equipped with sophisticated adiabatic calorimeters. In this article, it is shown that, when particular conditions are satisfied,[10] a set of three DSC runs is sufficient to gather reliable information useful both for interpolation and for extrapolation purposes. Based on the thermokinetic parameters determined a new procedure is presented that allows us to evaluate the adiabatic behavior of a thermal decomposition process with particular attention to the numerical assessment of the adiabatic onset temperature.

The kinetic modeling of a thermal process by means of a model fitting approach requires the identification[11,12] of the so-called kinetic triplet: $[A, E, f(\alpha)]$, where $f(\alpha)$ is the kinetic model, A is the preexponential factor, and E is the activation energy in an expression of the kinetic constant of the Arrhenius type[13]

$$K(T) = \mathrm{A}\ \exp\left(-\frac{E}{RT}\right) \tag{1}$$

The basic assumption that is considered valid is the so-called single step hypothesis,[14,15] which states that it is possible to write the reaction progress as the product of two independent terms, the first depending only on the temperature and the second exclusively depending on the conversion α

$$\frac{d\alpha}{dt} = K(T)\ f(\alpha) \tag{2}$$

When using a semiempirical approach[10,16,17] (which allows us to lump in a simple kinetic model, the complex

Additional Supporting Information may be found in the online version of this article.

Correspondence concerning this article should be addressed to R. Sanchirico at E-mail: r.sanchirico@irc.cnr.it.

© 2013 American Institute of Chemical Engineers

kinetic behavior often observable during the thermal decomposition of a substance or during a runaway phenomenon), the choice of the kinetic models generally reduces to the reaction order n

$$\mathrm{RO}\,(n) : f(\alpha) = (1-\alpha)^n \tag{3}$$

and autocatalytic Sestak–Berggren model with exponents a and b

$$\mathrm{SB}\,(a,b) : f(\alpha) = \alpha^a (1-\alpha)^b \tag{4}$$

In dynamical DSC experiments, where the sample temperature is varied linearly and the specific heat power is measured, α is expressed as

$$\alpha = \frac{\int_0^t q(t)dt}{-\Delta H_{\mathrm{R}}} \tag{5}$$

with

$$-\Delta H_{\mathrm{R}} = \int_0^{\infty} q(t)dt = \frac{1}{\beta}\int_{T_O}^{T_{\mathrm{end}}} q(T)dT \tag{6}$$

It has been shown[10] that if a thermal decomposition process develops through a single peak event during a DSC dynamic run, two experiments carried out at different heating rate are sufficient to discriminate among the reaction order model RO(n) and the Sestak–Berggren (autocatalytic) SB(a,b) model. This discrimination procedure is summarized in Figure 1. In this figure, the heat power curves (Γ_1 and Γ_2) have been reported along with the corresponding conversions (α_1 and α_2) for two different DSC experiments carried out under dynamic conditions at the heating rates $\beta_1 < \beta_2$.

In the case of Figure 1A, the heat power curves show an intersection point $\Gamma_1 \cap \Gamma_2$: this evidence allows us to conclude that the RO(n) model has to be ruled out and the application of the Sestak–Berggren model should provide $0 < a < 1$ and $b > 0$. On the other hand, in Figure 1B the case has been reported for which the heat power curves do not show any intersection points (if not at the origin): this circumstance allows to exclude an autocatalytic behavior (SB(a,b) model) and suggests the validity of the RO(n) model.

The introduction of suitable variables calculated considering the experimental heat power and conversion curves and their successive linear interpolation allows the assessment of a first estimate of the reaction exponents (n in the case of reaction order or (a, b) in the case of the Sestak–Berggren model). A third run carried out at a heating rate β_3 different than β_1 and β_2 allows the validation of the results with respect to the reaction order(s) [applying the procedure above to the different combinations of curves generated with the data collected at heating rates (β_2, β_3) and (β_1, β_3) other than (β_1, β_2)] and provides, by means of the application of the extended Kissinger's method, a first estimate of the Arrhenius parameters. The final values of the parameters are determined with a multivariate nonlinear fitting procedure performed considering all the three DSC dynamic runs and the initial values of the parameters previously determined. The procedures discussed above will be shortly illustrated in discussion section and is described in detail in Ref. 10.

Once determined, the kinetic triplet can be adopted also for extrapolation purposes. The possibility of gathering

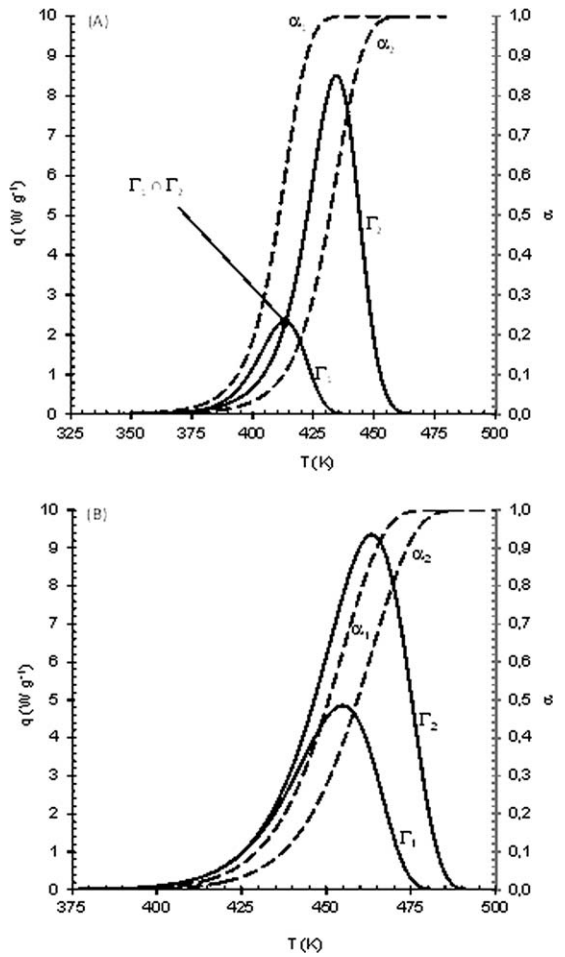

Figure 1. Heat power curves (Γ_i, $i = 1, 2$; solid curves/left scale) and the corresponding conversions (α_i, $i = 1, 2$; dashed curves/right scale) at two different heating rates (β_i, $i = 1, 2$; $\beta_1 < \beta_2$) as a function of the temperature in the case of an autocatalytic behavior described by the SB(a,b) model (A) and a Reaction Order RO(n) model (B).

reliable information under adiabatic conditions is fundamental in the context of a safety analysis. The most important critical parameters should be measured by means of experiments that involve the use of sophisticated adiabatic calorimeters.

To illustrate the procedures that will be discussed later, a short description follows on how a real adiabatic calorimeter works, the data that it is possible to collect and the possible drawbacks is in order.

In a classic Heat–Wait–Search (HWS) experiment performed using the ARC calorimeter[18] (for example), the sample is filled in the reactor (bomb) made of different materials (Stainless Steel, Hastelloy C, Titanium, etc). The system is brought to an initial temperature well below its thermal instability window. Then, a series of HWS cycles are performed until (if it exists) an *exotherm* is detected. During an HWS cycle, the sample is heated to the next temperature (*Heat*) by a preselected heat step temperature (usually 2.5–25 K). After this a *Wait* phase, whose length is also selected by the user (generally 5–10 min), allows the instrument to be equilibrated at the new temperature. This phase is

followed by a *Search* window in which the measured heat rate is continuously monitored and compared to a preselected (by the user) heat threshold (generally equal to 0.02 K min^{-1} but other values are also possible). If the experimental heat rate is greater than the heat threshold, the calorimeter switch in adiabatic mode (the corresponding temperature is the adiabatic onset temperature) and the process is monitored in these conditions until the end.

From this description, it is clear that the adiabatic behavior of the system is intimately related to the instrumental parameters in addition to the physical and thermokinetic characteristics of the reacting system. In particular, a physical parameter that plays a fundamental role is the so-called thermal inertia[19] defined as

$$\phi = 1 + \frac{m_b C_{P,b}}{m_S C_{P,S}} \tag{7}$$

where m_S is the mass and $C_{P,S}$ is the specific heat of the sample and m_b is the mass and $C_{P,b}$ is the specific heat of the bomb. In an adiabatic experiment, this is one of the most important parameter that affects the behavior of the system. For the extrapolation of the results to the industrial scale, its value should be kept as close as possible to one. However, this requirement sometimes is difficult to realize. Let us consider, for example, a test involving an explosive. For safety reasons, it is likely that the experiments will be performed with very large values of the thermal inertia (5–20 are not strange values). Moreover, due to the large sample mass or its particular reactivity, when using a pressure compensated calorimeters (such as Phitec II, VSP2, APTAC, etc) that in particular conditions allow us to realize experiments with very low value of the thermal inertia, the pressure rate can exceed the instrument limits with possible damage of the device. Other limitations of real adiabatic calorimeters are related to the temperature control mechanism. It has been reported, for example, that when using an accelerated rate calorimeter (but these considerations are easily extended to other type of adiabatic calorimeters without a mixing device) the temperature gradients inside the sample could affect the experimental results.[20] Furthermore, the adiabatic conditions can be lost (this is particularly true for the oldest devices while modern adiabatic calorimeters allow to track very fast exothermic events up to 200 K min^{-1}) if the heat rate exceeds some limits.[21] Indeed, adiabatic techniques have their advantage if compared to other experimental approaches. For example, adiabatic calorimeters are generally equipped with pressure measurement systems which provide key information for the design of venting systems. At the end, we can conclude that the most reliable approach should include different experimental techniques. DSC data can be used to derive reliable thermokinetic information which can be used to model the system under study, validate the adiabatic data or help us when particular circumstances prevent the direct acquisition of real information.

If a thermal decomposition's process is described by a given kinetic triplet with reaction heat calculated using Eq. 6, the energy balance that holds under adiabatic conditions is

$$\varphi \; m_S \; C_{P,S} \frac{dT}{dt} = K(T) f(\alpha)(-\Delta H_R) \tag{8}$$

with $K(T)$ evaluated using Eq. 1 and ϕ using Eq. 7. Thus, in adiabatic conditions, where the unknown functions are the temperature and the conversion degree α, the problem that has to be solved is the ordinary differential problem consisting in Eqs. 2 and 8 with the following initial conditions: at $t = 0$, $T(0) = T_0$, and $\alpha(0) = \alpha_0$.

Adiabatic onset temperature calculation

Adiabatic onset temperature at the present stage of knowledge can be assessed by means of the use of adiabatic calorimeters. In the procedure proposed by the author this key safety parameter is estimated starting from the knowledge of the thermokinetic parameters of the thermal decomposition of the process under study, which are derived from a suitable set of dynamic DSC runs. The analysis of a real adiabatic experiment carried out in HWS modality shows that the adiabatic onset temperature depends on the thermal history of the sample, on the heat rate threshold chosen to detect the exotherm and on the characteristic of the system under study (sample and bomb characteristics).

The thermal history which has been taken into account to develop the algorithm we are going to describe considers a dynamic linear heating of the sample at a heating rate γ starting from an initial temperature $T_{Start.}$ The numerical integration of Eq. 2 over a predetermined temporal grid—starting from zero and increasing the final integration time by a prefixed temporal step Δt—allows the assessment of the conversion degree $\alpha_{i,dyn} = \alpha_{dyn}(T_i)$ at the dynamic temperature $T_i = T_{i-1} + \gamma \Delta t = T_{START} + i\gamma\Delta t$; at the end of each step, these two values are used as initial conditions to integrate the system of Eqs. 2 and 8 (adiabatic simulation) assigning as initial adiabatic conversion ${\alpha^{(0)}}_{i,ad} = \alpha_{i,dyn}$ and as initial adiabatic temperature: ${T^{(0)}}_{i,ad} = T_{i,dyn}$; the numerical solution determined in this way allows the assessment of the heat rate $\left(\frac{dT}{dt}\right)_{ad,i}$ at the beginning of the adiabatic process evaluated adopting the previous initial conditions. The calculated adiabatic onset ($T_{0,Calc}$) is determined as the temperature at the end of the nth iteration for which, given a reference heat threshold ζ, the termination criterion $\left(\frac{dT}{dt}\right)_{ad,n} > \zeta$ is satisfied.

Once the adiabatic onset temperature is determined, the whole adiabatic behavior of the substance can be assessed by means of the integration of the system of Eqs. 2 and 8 considering $T_{0,calc}$ and the corresponding $\alpha_0 = \alpha(T_{0,Calc})$ as initial conditions. The iterative procedure described above will be implemented in the next section considering as a practical example the thermal decomposition of dicumyl peroxide (DCP) (source code is available as Supplemental Material).

Results and Discussion

Materials and methods

DCP (molecular weight: 270.37, CAS number: 80-43-3) at ambient conditions is a white crystalline powder that was purchased from Sigma-Aldrich (98 w/w-% purity). This substance is an organic peroxide of industrial importance used as initiator in different polymerization processes, as cross-linking or curing agent. A number of severe accidents due to its thermal decomposition have been reported during a recent past and this despite its common use and the efforts devoted to characterize the kinetics involved during its thermal decomposition process.[22–26] A literature survey shows that the thermal decomposition of pure crystalline DCP is a strong exothermal process that develops with large gas and heat evolution following an apparent reaction order kinetic.[22–28] Table 1 reports the thermokinetic parameters

Table 1. Thermokinetic Parameters Reported in the Literature for the Thermal Decomposition of DCP

Ref.	A (s^{-1})	E (kJ mol^{-1})	n	$-\Delta H_R$ (J g^{-1})
22	$6.41 \times 10^{+14}$	130	1	740
23	–	–	–	993 ÷ 992
24	$6.41 \times 10^{+14}$	132	1	741
25	$3.19 \times 10^{+15}$	124.58	1	744.85
26	$(1.29 \div 8.63)\ 10^{+15}$	132 ÷ 139	0.85 ÷ 1.0	666 ÷ 813
27	$6.41 \times 10^{+14}$	132	1	740
28	$(4.26 \pm 0.06)\ 10^{+13}$	132 ± 2	1.01 ± 0.1	860.3

found in the literature cited for the thermal decomposition of DCP.

The thermal decomposition process of DCP involves a complex reaction network which is triggered by the homolytic breaking of the oxygen–oxygen bond. The radical chain propagation that follow leads to the formation of different termination products such as acetophenone, dimethyl phenyl carbinol, and cumyl methyl ether in the condensed phase and CH_4, C_2H_6 C_2H_4 in the gas phase.[28] If a semiempirical approach is taken a strong simplifying hypothesis that is considered is represented by the Eq. 2 (single step hypothesis). This means that the behavior of the system under study can be explained "lumping" in a single process its complex nature.[10,14,15] It has to be stressed that although the lumped models are generally accurate often the physical meaning of the detailed reactions that really occur can be lost.

An experimental study has been conducted to test the approach discussed above. It has been organized with the following logic: a set of three dynamic runs were performed with the aim of identifying the model $f(\alpha)$, the Arrhenius parameters and the heat of decomposition; once estimated, these parameters have been employed for the simulation of the system's behavior considering different calorimetric conditions and the results have been compared with the experimental data coming from a set of real DSC and adiabatic runs.

DSC Experiments. DSC runs have been performed using a PerkinElmer DSC 8000 calorimeter equipped with an Intracooler II cooling system. Baseline calibration has been performed over 253–673 K temperature range. As calibration standards indium (expected temperature and fusion heat are equal to 429.76 K and 28.45 J g^{-1}, respectively) and lead (expected temperature and fusion heat are equal to 600.63 K and 23.01 J g^{-1}, respectively) have been used. Dynamic runs have been carried out on samples of approximately 2.1–2.9 mg using high pressure capsules (PerkinElmer part n.B018 2901 capable to withstand up to 10^7 Pa of internal pressure) and adopting temperature ramps started (in all cases) at 263 K with different heating rates (1.5, 2.5, 5.0, 10.0, 12.5, 20.0, and 40.0 K min^{-1}). The experimental conditions as well as the principal results gathered in the course of these runs are reported in Table 2.

Table 2. Experimental Conditions and Principal Results Gathered During the Dynamic DSC Runs Carried Out on DCP

Run	β (K min^{-1})	m_S (mg)	T_{max} (K)	$-\Delta H$ (J g^{-1})
1	2.5	2.7	437.1	951.0
2	10.0	2.8	454.5	908.5
3	20.0	2.6	463.4	937.8
A	1.5	2.5	434.7	1033.9
B	1.5	2.5	433.5	809.4
C	5.0	2.6	443.9	924.0
D	12.5	2.9	454.9	926.6
E	40.0	2.1	470.3	895.6

Runs 1, 2, and 3 have been used for identification; Runs A–E have been considered for the extrapolation's verification.

Isothermal DSC experiments have been performed at different temperatures (418, 423, 428, 433, and 443 K) using the same capsules used for the dynamic experiments with samples of 2.5–2.8 mg. In all cases, the samples have been heated to the desired temperature staring also in this case from 263 K with a controlled heating rate of $\beta = 10$ or 20 K min^{-1}. The principal conditions adopted to carry out these runs have been reported in Table 3. The values of the conversion degree at the end of the heating phase are reported in the last column of this table and have been calculated considering the data of the dynamic runs 2 and 3 of Table 2. The heat of decomposition calculated considering the runs 1, 2, 3, and using Eq. 6 was $-\Delta H_R = 932.4 \pm 21.7$ J g^{-1} and its mean value has been used in all the subsequent calculations.

Adiabatic Experiments. These experiments have been performed by means of an accelerating rate calorimeter by Columbia Scientific Industries (Austin, TX). All the runs have been performed using the same Hastelloy C bomb (mass = 15.1938 g and $C_{P,b} = 0.42$ J g^{-1} K^{-1}). This bomb has been recovered at the end of each run, cleaned carefully and reused in the successive experiments. Once prepared, the bomb was mounted inside the calorimeter and the experiment performed by setting via remote control all the necessary parameters: these were, the initial starting temperature (T_{START}), the heat rate threshold (slope sensitivity), the heat step temperature, and the wait time (equal to 10 min in all the cases). Specific heat of the sample was considered equal to:[29] $C_{P,S} = 1.909$ J g^{-1} K^{-1}. The instrumental conditions adopted along with the principal characteristic of the systems are summarized in Table 4.

Identification of the model

Figure 2 shows the results gathered during the DSC dynamic runs 1, 2, and 3 of Table 2.

These curves have been considered with the goal of identifying the kinetic model and of determining the Arrhenius parameters concerned with the thermal decomposition of DCP. The curves were corrected by subtracting from the

Table 3. Experimental Conditions Adopted to Carry Out the Isothermal Runs Performed on DCP

Run	β (K min^{-1})	m_S (mg)	Temperature (K)	α_O
1	10	2.6	418	0.0459
2	10	2.8	423	0.0720
3	10	2.5	428	0.1078
4	10	2.8	433	0.1559
5	20	2.5	443	0.1543

Table 4. Instrumental Parameters and Experimental Conditions Adopted for the Adiabatic ARC Runs Carried Out on DCP

Run	T_{START} (K)	Heat step temp. (K)	Slope sensitivity (K min^{-1})	m_S (g)	ϕ
1	333	5.0	0.020	1.3562	3.46
2	333	5.0	0.010	2.0922	2.59
3	348	2.5	0.010	1.9541	2.71

experimental DSC raw signals, the corresponding baselines evaluated using the tangential area proportional method. An example of this chain calculation is reported in Figure 3.

Since the analysis of the Figure 2 does not show evident intersection points among all the possible combinations of distinct curves, it can be concluded that among the Sestak–Berggren and the Reaction order the last is the model suitable for describing the system.

It has been demonstrated[10] that a first estimate of the exponent n can be obtained by means of the linear interpolation of the following variables

$$\ln\left(\frac{q_i}{q_j}\right) \quad \text{vs.} \quad \ln\left(\frac{1-\alpha_i}{1-\alpha_j}\right) \tag{9}$$

where the indexes $i = 1\ldots3$, $j = 1\ldots3$ ($i \neq j$) refer to the first three runs of Table 2.

As shown in Figure 4—which refers to the couple of DSC runs performed on DCP in dynamic condition at heating rate β_2, and β_3 (second line of Table 5)—the points taken into account (gray rectangle) for the calculation of the variable reported in Eq. 9 do not consider the tails.[10] In fact, if two curves are *too close* (as it is evident, if we consider by visual inspection the highly dispersed behavior of the values reported for $\ln\left(\frac{q_2}{q_3}\right)$ vs. T on the tails) due to the nonlinear transformations involved, the experimental errors could amplify thus leading to a poor evaluation of these variables.

Although the visual inspection of these curves provides a practical tool for the assessment of the temperatures evaluation range, a quantitative criterion (not developed yet) would be in order to determine a more objective result independent from the choices of the user.

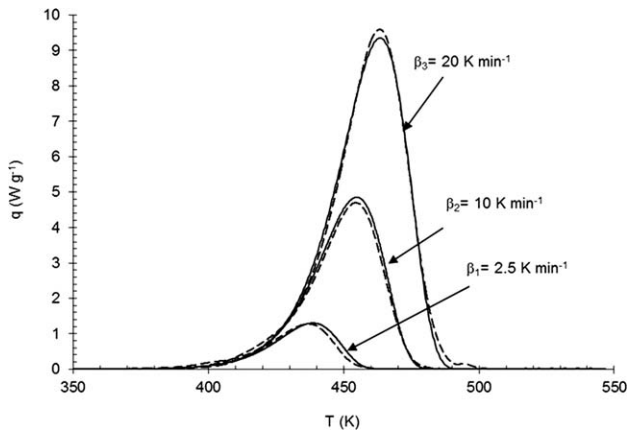

Figure 2. Calculated (solid) and experimental (dashed) heat powers obtained during a set of DSC dynamic runs carried out on DCP at different heating rates (Runs 1, 2, and 3 of Table 2).

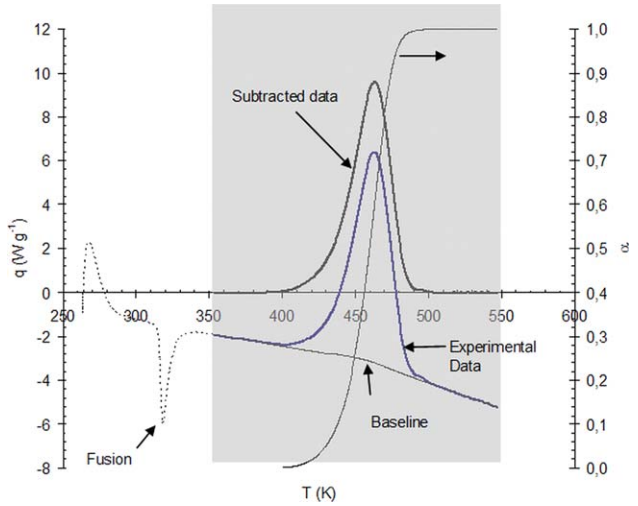

Figure 3. Chain calculations carried out on Run 3 of Table 2—Gray area has been used for data extraction.

[Color figure can be viewed in the online issue, which is available at wileyonlinelibrary.com.]

As shown in Figure 5, the points $\ln(q_2/q_3)$ vs. $\ln[(1-\alpha_2/(1-\alpha_3)]$ evaluated over the "temperature interval" previously determined have been linearly interpolated thus obtaining the estimation of n for the curves collected at the heating rates β_2 and β_3.

The results of these interpolations performed for all the possible combinations of curves along with the linear regression coefficients and the temperature evaluation ranges adopted have been reported in Table 5. These results allowed the determination of an initial estimate for the reaction order equal to: $n_0 = 0.89 \pm 0.15$.

Extended Kissinger's method[30] has been applied considering Eq. 10.

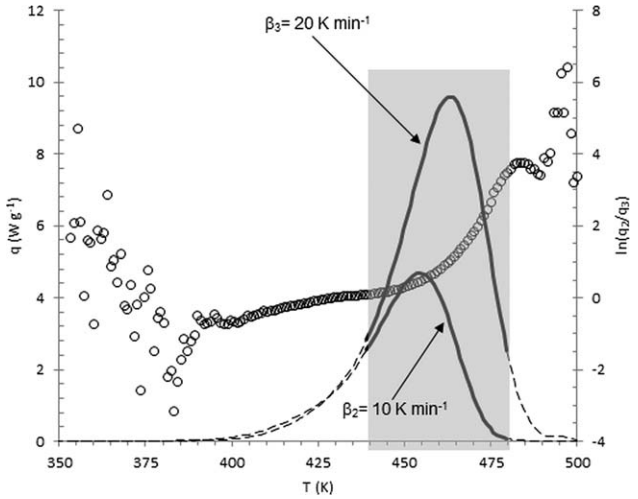

Figure 4. Temperature's interval selection for the assessment of the first estimate of the reaction order *n* considering the dynamic DSC curves collected during the thermal decomposition of DCP at 10 and 20 K/min (cf. second raw of Table 5).

Shadowed rectangle corresponds to the points considered for the calculations.

Table 5. Experimental Combination of Curves Considered for the Initial Estimation of the Reaction Order *n*

Data sets at	Evaluation temperature range	R^2	n
β_1, β_2	430–446	0.9588	0.76
β_2, β_3	439–480	0.9894	1.05
β_1, β_3	420–452	0.9751	0.86
		Mean value	0.89

$$\ln\left(\frac{\beta_i}{T_{i,\max}^2}\right)=-\frac{E}{RT_{i,\max}}+\ln\left(\frac{AR}{E}\varphi_O\left(\alpha_{i,\max}\right)\right)\qquad(i=1,2,3)\tag{10}$$

where $\varphi_O\left(\alpha_{i,\max}\right)=-D\left[f\left(\alpha_{i,\max}\right)\right]$. Considering the temperature at the maximum $T_{\max,i}$ (see Table 2) for the different heating rates β_i, the linear interpolation of $\ln\left(\frac{\beta_i}{T_{\max,i}^2}\right)$ vs. $\frac{1}{T_{\max,i}}$ allowed the determination of an activation energy equal to $E_0=125{,}870$ J mol^{-1} and a preexponential factor of $A_0=3.64\ 10^{+12}\cdot s^{-1}$. The derivative of $f(\alpha)$ necessary for the determination of the preexponential factor, that in the case of RO(n) model is: $D(f(\alpha))=-n(1-\alpha)^{n-1}$, has been evaluated considering the value of the reaction order $n_0=0.89$ previously estimated.

The vector $[A_0, E_0, n_O]$ has been used as initial estimate in an identification procedure that allowed the assessment of the kinetic model $f(\alpha)$ and of the Arrhenius parameters A and E. All the calculations have been performed by means of the software Matlab.[31] The final estimate of the thermokinetic parameters has been assessed by means of the least mean square fit evaluated considering all the data collected at the different heating rates.[10,32]

Due to the extreme stiffness of the optimization of the Arrhenius parameters A and E, a reparametrized expression of the kinetic constant has been used[10,33–35]

$$K(T)=\exp\left[r-d\frac{E_0}{R}\left(\frac{1}{T}-\frac{1}{T_{\mathrm{Ref}}}\right)\right]\tag{11}$$

where $T_{\mathrm{Ref}}=451.7$ K is a reference temperature calculated as the mean value between the temperature at the first inflection point of the peak at lowest heating rate β_1 and the temperature at the second inflection point at the highest heat rate β_3. With this assumption, the new parameter's vector that should be identified is $\vartheta'=[r,d,n]$. The initial estimate $\vartheta'_0=[r_0,d_0,n_0]$ is calculated starting from the original parameters A_0, E_0, setting $d_0=1$, and deriving r_0 by means of the following transformation

$$r_0=\ln(A_0)-\left(\frac{E_0\ d_0}{R\ T_{\mathrm{Ref}}}\right)\tag{12}$$

The initial values of the centered and scaled Arrhenius parameters along with the initial estimate of the exponents of the reaction order n adopted in the successive optimization procedure resulted in: $r_O=-4.60$, $d_O=1.0$, and $n_O=0.89$. After the optimization performed considering these initial values, the following values have been determined: $\hat{r}=-4.59$, $\hat{d}=1.06$, and $\hat{n}=0.93$ from which, considering the following inverse transformations

$$\hat{E}=\hat{d}E_0\tag{13}$$

$$\hat{A}=\exp\left(\hat{r}+\frac{E_0\ \hat{d}}{R\ T_{\mathrm{Ref}}}\right)\tag{14}$$

the vector of parameters $\hat{\vartheta}=\left[\hat{A},\hat{E},\hat{n}\right]$ has been assessed.

For gathering inferential information about the identified parameters these have been reoptimized removing their centering and scaling, that is, starting from these final estimates and using for Eq. 1 to express $K(T)$. This procedure allowed (Matlab command: *nlparci*[31]) the calculation of the 95% confidence intervals for the estimated parameters. These results were reported in Table 6, while the calculated curves along with the corresponding experimental data are given in Figure 2.

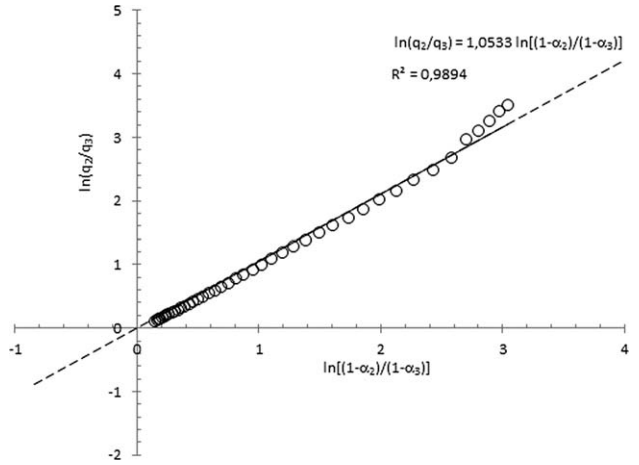

Figure 5. ln(q_2/q_3) vs. ln[$(1-\alpha_2/(1-\alpha_3)$] determined over the temperature interval reported in Figure 4 along with the corresponding regression line.

Table 6. Final Estimate of the Arrhenius and RO(n) Model Parameters Along With Their 95% Confidence Intervals

Parameter	Mean value	95%—Left error bound	95%—Right error bound
$\hat{A}\left(s^{-1}\right)$	$3.10\times10^{+13}$	$3.06\times10^{+13}$	$3.14\times10^{+13}$
$\hat{E}\left(\mathrm{Jmol}^{-1}\right)$	133,892	133,835	133,950
$\hat{n}$	0.93	0.92	0.94

Experimental verification

A series of DSC runs carried out both in dynamic (Runs A–E of Table 2) and isothermal conditions (Table 3) along with a set of runs carried out using the accelerating rate calorimeter (Table 4) have been analyzed to prove that the model and the Arrhenius parameters identified in the last section can be considered to describe the thermal behavior of the system with sufficient reliability.

Dynamic DSC Results. Figures 6 and 7 show the experimental heat powers and the corresponding calculated curves obtained integrating [Matlab solver ODE 15s (Stiff/NDF)[31]] the Eq. 2, with $q=\frac{d\alpha}{dt}(-\Delta H_R)$ and considering temperature

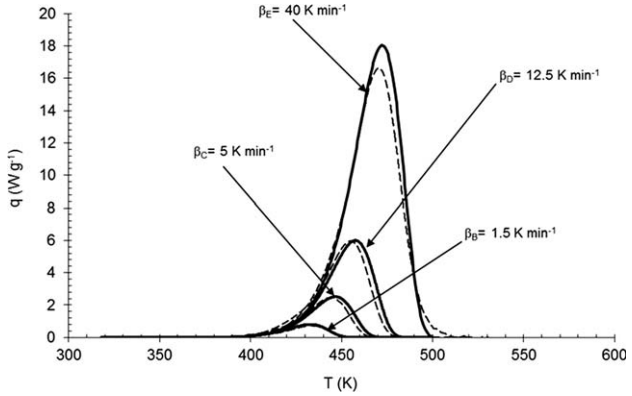

Figure 6. Calculated curves obtained using the parameters reported in Table 6 (solid) and experimental (dashed) results obtained during a set of Dynamic DSC runs carried out on DCP (runs B to E of Table 2).

ramps given by $T(t)=T_0+\beta t$ (with $\beta=\beta_A\ldots\beta_E$, and $\alpha_0=0$ at $T_0=263$ K in each case) and the values of the parameters reported in Table 6.

An analysis of these figures points out that the calculated curves are compatible with the experimental results collected during the runs A–E (see Table 2) that were not used for the identification of the parameters.

Isothermal Results. In Figure 8 is reported the raw instrumental signal, the baseline and the corresponding subtracted signal (left scale) along with the temperature history (sample temperature, right scale) for the Run 4 of Table 3. The experimental baselines have been acquired resubmitting to the same thermal history, the samples recovered at the end of the isothermal phase and submitted to a quenching procedure. These baselines have been subtracted to the first signal and the subtracted curves have been considered for the successive calculations. Gray area highlights the segment of the run concerned with the isothermal phase.

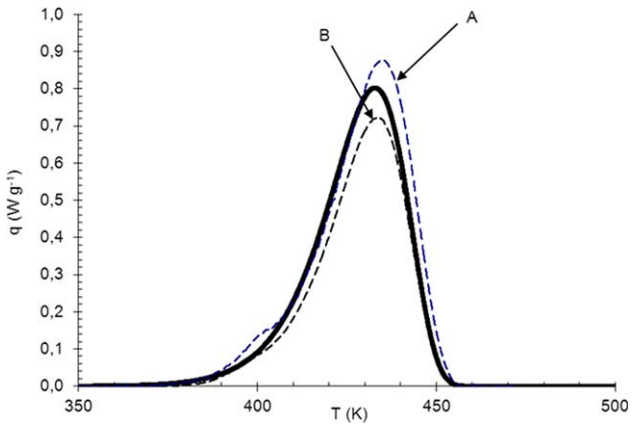

Figure 7. Experimental specific heat powers (dashed curves) gathered in two different dynamic experiments carried out on DCP at 1.5 K/min (Runs A and B of Table 2) and calculated values (Solid curve) obtained using the kinetic parameters reported in Table 6.

[Color figure can be viewed in the online issue, which is available at wileyonlinelibrary.com.]

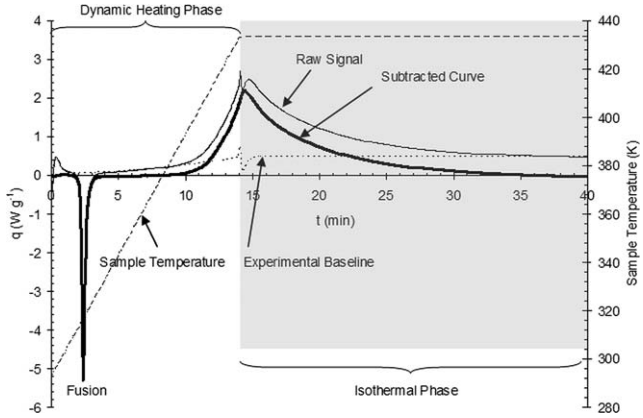

Figure 8. Signal extraction procedure carried out considering the data gathered at 433 K (Run 4 of Table 3).

Gray area highlights the zone considered for the successive calculations (Isothermal Phase).

From the heat power signals determined using the last procedure, after numerical integration (Matlab command *trapz*[31]) the conversion curves reported in Figure 9 have been obtained.

In this figure, it is reported that the numerical integration of Eq. 2 carried out at different temperatures using for the initial conversion α_0, the value reported in the last column of Table 3 and for the kinetic parameters the identified values (mean values) reported in Table 6. Also in this case, a good agreement among the calculated and experimental values is shown. It is worth to stress that particular care should be paid when considering isothermal DSC data especially in respect to the possibility of activation of secondary reactions which could be masked under these conditions also over very long reaction times.

Adiabatic Results. To verify that the results gathered considering the kinetic model identified using the dynamic DSC runs can be extrapolated also in adiabatic conditions and test the algorithm developed for the estimation of the onset temperature, the results of a series of experiments carried out on DCP using an accelerated rate calorimeter have

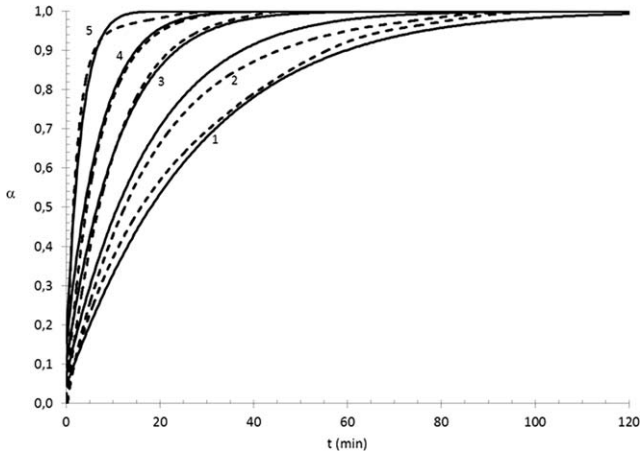

Figure 9. Calculated (solid) and experimental (dashed) conversions obtained during a set of isothermal DSC experiments carried out on DCP.

The numbers near the curves refer to the runs reported in Table 3.

Table 7. Principal Experimental Values Collected During the Adiabatic Runs of Table 4 Carried Out on DCP

Run	$T_{0,exp}$ (K)	Heat rate at $T_{0,exp}$ (K)	$\Delta T_{ad,exp}$ (K)	$\tau_{ad,exp}$ (min)	P_{max} (bar)
1	369.23	0.030	121.14	322.26	16.11
2	364.18	0.019	149.39	478.30	26.67
3	361.38	0.012	146.21	758.86	24.34

been compared with the corresponding theoretical predictions.

The experimental conditions used to carry out these runs are reported in Table 4, while the principal results gathered during these runs are summarized in Table 7.

As an example, in Figure 10 are reported the results gathered during the run 2 of Table 4. The gray area on the left of this figure shows the HWS steps that the ARC performed until the detection of the exotherm that resulted at the temperature $T_{O,exp}$ (with a corresponding heat rate at $T_{0,exp}$ reported in the third column of this table). The other values of this table refer to the experimental adiabatic temperature rise ($\Delta T_{ad,exp}$), the time to maximum rate evaluated at the onset ($\tau_{ad,exp}$), and the maximum pressure (pressure at $T = T_{0,exp} + \Delta T_{ad,exp}$). The points that belong to the HWS phase have been then linearly interpolated to derive the heating rate γ. These values were then considered to define the heating ramps [$T(t) = T_{START} + \gamma t$] adopted for the assessment of the adiabatic onset temperatures by means of the method described in *Adiabatic onset temperature calculation* section.

In Table 8, the conditions (start temperature T_{START} and heat rate of the heating ramp γ) adopted to determine the calculated onset temperatures $T_{0,calc}$ as well as the other critical adiabatic parameters have been reported. The termination of the iterative procedure has been controlled by choosing as heat rate threshold the initial adiabatic rate found experimentally and reported in the third column of Table 7.

In Figure 11, the experimental data (HWS phase not shown) concerned with the runs of Table 4 have been

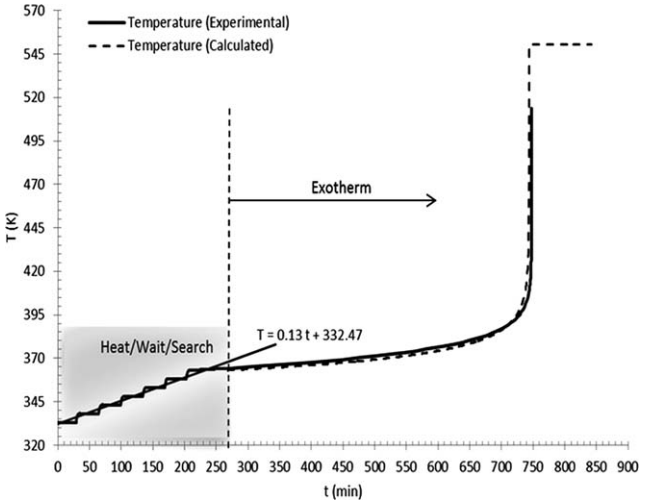

Figure 10. Adiabatic ARC data [experimental (solid curve) and calculated (dashed curve)] of the thermal decomposition of DCP (Run 2 of Table 4).

Gray area highlights the heat/wait/search phase before the detection of the adiabatic onset.

Table 8. Calculated Values and Conditions Adopted for the Assessment of the Adiabatic Onset and Time to Maximum Rate

Run	T_{START} (K)	γ (K min^{-1})	$T_{0,calc}$ (K min^{-1})	$\Delta T_{ad,calc}$ (K)	$\tau_{ad,calc}$ (min)
1	333	0.20	369.29	140.10	318.00
2	333	0.13	363.07	187.30	474.37
3	348	0.06	359.70	179.32	737.50

reported along with the calculated curves (linear heating phases not shown) evaluated considering the proposed procedure and adopting the kinetic parameters reported in Table 6,

In Table 9, it has been reported the error $\varepsilon = \frac{\text{Experimental value} - \text{predicted value}}{\text{Experimental value}} \times 100$ evaluated considering the experimental (Table 7) and the calculated values (Table 8) both for the adiabatic onset temperature and time to maximum rate.

Also in this case, the analysis of the data reported in Tables 7–9 indicates a good agreement among the experimental and calculated adiabatic data.

Conclusions

It has been confirmed that when a thermal event is represented by a single peak in a DSC dynamic run, reliable information can be gathered from three dynamic experiments carried out at different heating rate. In particular, the geometric characteristic of these curves allow us to discriminate among SB(a,b) and RO(n) kinetic. A suitable identification procedure allowed in the case of DCP the assessment of the thermokinetic parameters of its thermal decomposition process. For this compound, the kinetic triplet has been determined considering a set of DSC dynamic runs carried out at 2.5, 10, and 20 K min^{-1}. This substance has been confirmed to decomposes exothermically ($-\Delta H_R = 932.4 \pm 21.7$ J g^{-1}) following a reaction order kinetic with $n = 0.93 \pm 0.02$ and with the following values of the Arrhenius parameters: $A = (3.10 \pm 0.81)\ 10^{+13}$ s^{-1}; $E = 133{,}892 \pm 114$ J mol^{-1}.

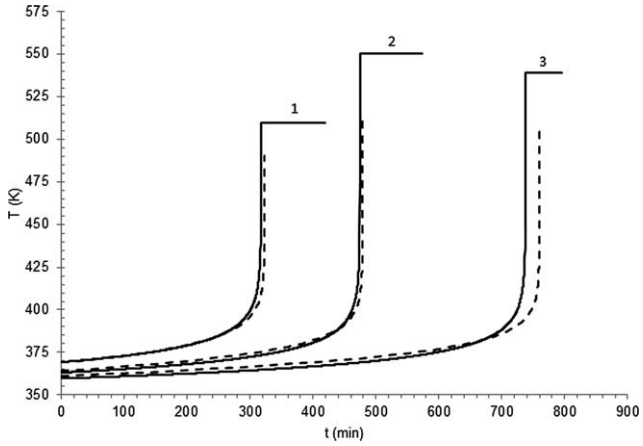

Figure 11. Adiabatic ARC data [experimental (dashed) and calculated (solid curve)—times have been scaled considering the instant at which the exotherm has been detected] of the thermal decomposition of DCP.

The numbers near the curves refer to the runs reported in Table 4.

Table 9. Errors Between Calculated and Experimental Values for the Adiabatic On Set Temperature T_O and Time to Maximum Rate τ Concerned With the Thermal Decomposition of DCP

Run	ε_{To} (%)	ε_{τ} (%)
1	−0.02	+1.3
2	+0.30	+0.8
3	+0.47	+2.8

These values, which are compatible with those reported in the literature (see Table 1), have been used with the aim of simulating the system behavior outside the experimental conditions adopted for their identification (extrapolation); the results of these simulations exhibit a satisfactory agreement with the corresponding experimental results. In particular, an iterative procedure has been developed and proved to allow the assessment of the adiabatic onset temperature along with the global adiabatic behavior of the system under study. It is worth to observe that DSC techniques should be considered with caution and the method proposed for the estimation of the adiabatic onset temperature should be intended only as a raw estimate of this key safety parameter. The approach proposed in the article is not intended to replace the existing adiabatic techniques, rather it should be considered as a supplemental tool devoted to validate and integrate the experimental real adiabatic data. It should be highlighted that the proposed approach could be applied without substantial modification also in the case of autocatalytic processes. In the latter case, the difference would arise only in the model better describing the DSC dynamic data [SB(a,b) instead of RO(n)].

Acknowledgments

The author would like to dedicate this work to his wife Isabella and the two little "earthquakes" Angela and Anna Chiara, to his mother Enza and his brother Stefano.

Notations

Roman letters

A = preexponential factor, min^{-1}
ARC = adiabatic rate calorimeter
d = parameter in Eq. 11
D = derivative of a function
DCP = dicumyl peroxide
DSC = differential scanning calorimeter(try)
E = activation energy, J mol^{-1}
HWS = heat-wait-search phase in an ARC run
N = number of runs
r = parameter in Eq. 11
R = 8.314 = universal gas constant, J $K^{-1}mol^{-1}$
RO(n) = reaction order kinetic with reaction order n
SB(a,b) = autocatalytic Sestak–Berggren model with exponents a and b
t = time, min or s
T = temperature, K
T_O = adiabatic onset temperature, K

Greek letters

α = conversion, dimensionless
β = heating rate in a DSC dynamic run, K min^{-1}
ε = error, dimensionless
γ = heating rate as the result of the interpolation of the HWS, K min^{-1}
ζ = reference heat threshold, K min^{-1}
θ = parameter's vector
τ = adiabatic time to maximum rate, min
Γ = heat power curve
ΔH_R = reaction heat, J g^{-1}
ΔT_{ad} = adiabatic temperature rise, K

Subscripts and other symbols

ad = adiabatic conditions
calc = calculated value
dyn = dynamic conditions
exp = experimental value
0 = initial value (or condition)
$\cap$ = intersection between sets

Literature Cited

1. Giby J. Recent reactive incidents and fundamental concepts that can help prevent them. *J Hazard Mater.* 2003;104:65–73.
2. Westerterp KR, Molga EJ. No more runaways in fine chemical reactors. *Ind Eng Chem Res.* 2004;43:4585–4594.
3. Brennan J, Kiihne GM. A little knowledge is a dangerous thing—unexpected reaction case studies make the case for technical discipline. *J Loss Prev Process Ind.* 2009;22:757–763.
4. Khan AA. Case histories and recent developments to improve safety assessments during process development. *Proc Saf Prog.* 2006;25(3):245–249.
5. Frurip DJ, Elwell T. Effective use of differential scanning calorimetry in reactive chemicals hazard evaluation. *Proc Saf Prog.* 2007;26(1):51–58.
6. Shanley ES, Melhem GA. A review of ASTM CHETAH 7.0 hazard evaluation criteria. *J Loss Prev Process Ind.* 1995;8(5):261–264.
7. Saraf SR, Rogers WJ, Mannan MS. Prediction of reactive hazards based on molecular structure. *J Hazard Mater.* 2003;98(1–3):15–29.
8. Gustin JL. Influence of trace impurities on chemical reaction hazards. *J Loss Prev Process Ind.* 2002;15:37–48.
9. Wei C, Saraf SR, Rogers WJ, Mannan MS. Thermal runaway reaction hazards and mechanisms of hydroxylamine with acid/base contaminants. *Thermochim Acta.* 2004;421(1–2):1–9.
10. Sanchirico R. Model selection and parameters estimation in kinetic thermal evaluations using semiempirical models. *AIChe J.* 2012;58(6):1869–1879.
11. Elder JP. The "E-ln(A)-f(α)" triplet in non-isothermal reaction kinetics analysis. *Thermochim Acta.* 1998;318:229–238.
12. Militký JZ, Sestak J. Building and statistical interpretation of non-isothermal kinetic models. *Thermochim Acta.* 1992;203:31–42.
13. Galwey AK. Eradicating erroneous Arrhenius arithmetic. *Thermochim Acta.* 2003;399:1–29.
14. Šimon P. Considerations on the single-step kinetics approximation. *J Therm Anal Calorim.* 2005;82:651–657.
15. Šimon P. The single-step approximation—attributes, strong and weak sides. *J Therm Anal Calorim.* 2007;88(3):709–715.
16. Màlek J, Criado M. Empirical kinetic models in thermal analysis. *Thermochim Acta.* 1992;203:25–30.
17. Burnham AK. Application of the Šesták–Berggren equation to organic and inorganic materials of practical interest. *J Therm Anal Calorim.* 2000;60:895–908.
18. Towsend DI, Tou JC. Thermal hazard evaluation by an accelerating rate calorimeter. *Thermochim Acta.* 1980;37:1–30.
19. Wilcock E, Rogers RL. A review of the phi factor during runaway conditions. *J Loss Prev Process Ind.* 1997;10(5–6):289–302.
20. Kossoy A, Sheinman I. Effect of temperature gradient in sample cells of adiabatic calorimeters on data interpretation. *Thermochim Acta.* 2010;500(1–2):93–99.
21. Tou C, Whiting LF. The thermokinetic performance of an accelerating rate calorimeter. *Thermochim Acta.* 1981;48:21–42.
22. Shen SJ, Wu SH, Chi JH, Lind CC, Horng JJ, Shu CM. Simulation of solid thermal explosion and liquid thermal explosion of dicumyl peroxide using calorimetric technique. *Simul Model Pract Theory.* 2011;19:1251–1257.
23. Hsu JM, Su MS, Huang CY, Duh YS. Calorimetric studies and lessons on fires and explosions of a chemical plant producing CHP and DCPO. *J Therm Anal Calorim.* 2012;217–218:19–28.
24. Wu SH, Shu CM. Reactive hazard analysis of cumene hydroperoxide and dicumyl hydroperoxide. *Proc Saf Prog.* 2010;29(2):162–165.
25. Lu KT, Chu YC, Chen TC, Hu KH. Investigation of the decomposition reaction and dust explosion characteristics of crystalline dicumyl peroxide. *Proc Saf Environ Protect.* 2010;88:356–365.

26. Wu SH, Shyu ML, I YP, Chi JH, Shu CM. Evaluation of runaway reaction for dicumyl peroxide in a batch reactor by DSC and VSP2. *J Loss Prev Process Ind*. 2009;22:721–727.
27. Shen SJ, Wu SH, Chi JH, Wang YW, Shu CM. Thermal explosion simulation and incompatible reaction of dicumyl peroxide by calorimetric technique. *J Therm Anal Calorim*. 2010;102:569–577.
28. Ben Talouba I, Balland L, Mouhab N, Abdelghani-Idrissi MA. Kinetic parameter estimation for decomposition of organic peroxides by means of DSC measurements. *J Loss Prev Process Ind*. 2011;24:391–396.
29. Duh YS, Wu XH, Kao CS. Hazard ratings for organic peroxides. *Proc Saf Prog*. 2008;27(2):89–99.
30. Llòpiz J, Romero MM, Jerez A, Laureiro Y. Generalization of the Kissinger equation for several kinetic models. *Thermochim Acta*. 1995;256:205–211.
31. Matlab, Software for Scientific Computing, Online Manuals and Additional Material, Available at: http://www.mathworks.com/. Last access on February 2013.
32. Opfermann J. Kinetic analysis using multivariate non-linear regression—I. *Basic concepts. J Therm Anal Calorim*. 2000;60:641–658.
33. Rodionova OE, Pomerantsev AL. Estimating the parameters of the Arrhenius equation. *Kinet Catal*. 2005;46(3):305–308.
34. Buzzi-Ferraris G. Planning of experiments and kinetic analysis. *Catal Today*. 1999;52:125–132.
35. Watts DG. Estimating parameters in nonlinear rate equations, *Can J Chem Eng*. 1994;72:701–710.

Manuscript received Sept. 24, 2012, and revision received Apr. 12, 2013.